

This is the accepted manuscript made available via CHORUS. The article has been published as:

Cooperative multiscale aging in a ferromagnet/antiferromagnet bilayer

S. Urazhdin and U. Danilenko

Phys. Rev. B **92**, 174416 — Published 19 November 2015

DOI: [10.1103/PhysRevB.92.174416](https://doi.org/10.1103/PhysRevB.92.174416)

Cooperative Multiscale Aging in a Ferromagnet/Antiferromagnet Bilayer

S. Urazhdin* and U. Danilenko

Department of Physics, Emory University, Atlanta, Georgia 30322, USA

Anisotropic magnetoresistance measurements show that the magnetization state in epitaxial $\text{Ni}_{80}\text{Fe}_{20}/\text{Fe}_{50}\text{Mn}_{50}$ bilayers exhibits aging over a wide range of temperatures and magnetic fields. The observed power-law time dependence indicates that aging is characterized by a wide range of activation time scales. Aging characteristics are also inconsistent with a superposition of independent activation barriers expected for Arrhenius-type relaxation. The observed effects indicate a fundamental connection with the critical phenomena in complex condensed matter systems.

PACS numbers: 85.70.Kh, 89.75.-k, 89.75.Da

In bilayers of materials with different lattice parameters, structural frustration can result in dislocations or even formation of amorphous interlayers¹. Similarly, magnetic frustration can be expected at interfaces between materials with different magnetic orders², originating from the random effective fields experienced by both materials due to the exchange interaction across their interface. In particular, some of the unusual magnetic properties exhibited by bilayers of antiferromagnets (AF) and ferromagnets (F) have been attributed to the magnetic domain walls that are formed to reduce the interfacial exchange energy^{3,4}, or even disordered spin states near the F/AF interface^{5,6}. After almost 60 years of extensive research, fundamental understanding of F/AF bilayer systems remains elusive. Besides theoretical challenges in describing the effective exchange fields at the F/AF interfaces, common experimental approaches, such as the hysteresis loop measurement, can lead to irreversible changes of the magnetic configuration, thus obscuring the essential signatures of frustrated systems such as aging⁷. Methods capable of magnetic characterization without varying the experimental parameters are needed to provide insight into the properties of these systems.

We utilized anisotropic magnetoresistance (AMR) to characterize the evolution of the magnetization state in F/AF bilayers without perturbing the system. Our measurements reveal power-law relaxation over a wide range of temperature T , indicating multiple scales of activation energies and activation times. The observed power-law form of relaxation is also independent of the prior magnetic history, demonstrating that aging is a cooperative process; it cannot be described in terms of independent activation barriers. These results provide a connection between the magnetic properties of F/AF bilayers and critical phenomena in complex systems.

Our samples were deposited by sputtering on annealed (0001)-oriented sapphire. An epitaxial (111)-oriented Pt(5) buffer layer was deposited at 550°⁸, followed by the F/AF bilayer $\text{Py}=\text{Ni}_{80}\text{Fe}_{20}(10)/\text{Fe}_{50}\text{Mn}_{50}(d)$ deposited at room temperature $T = 295$ K to avoid interdiffusion of the magnetic interfaces, and capped with $\text{SiO}_2(20)$ to prevent oxidation. All thicknesses are in nanometers (nm). The rms roughness of the films was less than 0.3nm, as verified by atomic force microscopy, and epi-

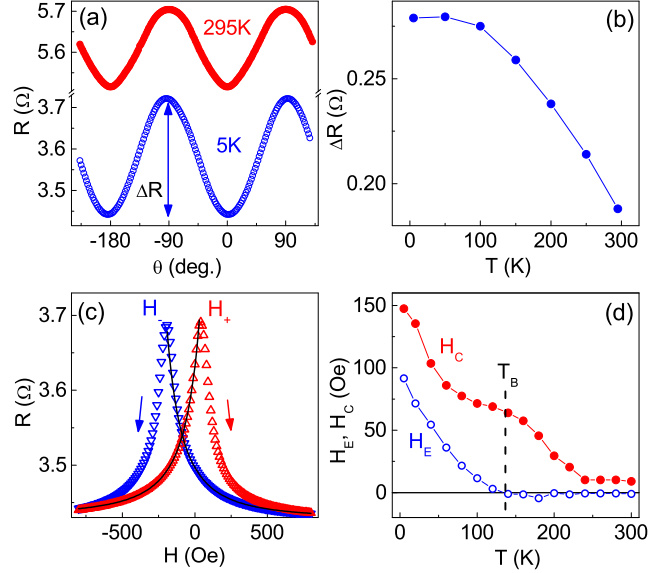


FIG. 1: (Color online) (a) Dependence of resistance on the in-plane orientation of H , at $T = 295$ K, $H = 100$ Oe (solid symbols), and 5 K, $H = 2$ kOe (open symbols). $\theta = 0$ is perpendicular to current. (b) Temperature dependence of magnetoresistance, determined from $R(\theta)$ obtained at $H = 2$ kOe, after initial field-cooling at $H = 500$ Oe, $\theta = 0$. (c) Magneto-electronic hysteresis loop obtained at 5 K, after four similar prior loops. Curves: fits based on the exchange field model described in the text. Coercive fields H_- and H_+ are labeled. (d) Coercivity H_C and exchange bias field H_E vs T .

taxy was confirmed by a combination of x-ray diffraction and magnetic anisotropy measurements⁹. We have fabricated and studied several samples with thickness d of FeMn ranging from 1 to 3.5 nm. Below, we focus on a sample with $d = 2$ nm, which exhibited an onset of exchange bias (EB)¹⁰ at $T_B = 140$ K, within the range $T = 5 - 300$ K accessible in our measurements.

Magnetoelectronic characterization was performed in the van der Pauw geometry, using an ac current $I = 0.1$ mA rms and lock-in detection. The resistance $R(\theta)$ exhibited a 180° -periodic sinusoidal dependence on the in-plane orientation of a sufficiently large field H [Fig. 1(a)]. The magnetoresistance $\Delta R = R(90^\circ) - R(0)$ determined at saturating $H = 2$ kOe exhibited a mono-

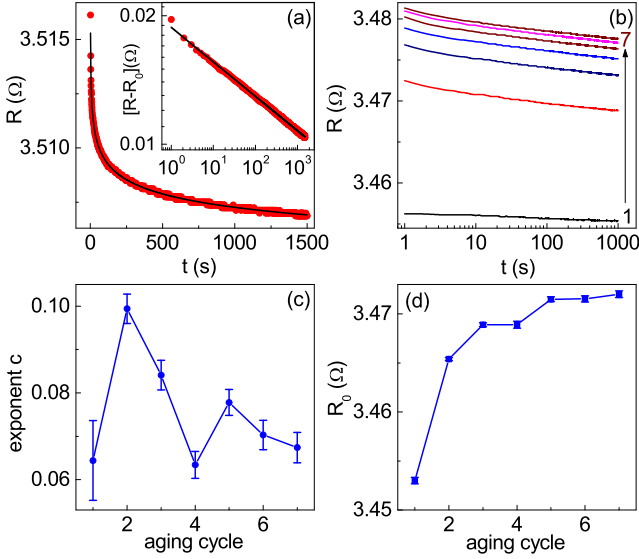


FIG. 2: (Color online) Aging at $T = 5$ K. (a) Symbols: time evolution of resistance R at $H_f = -300$ Oe, after prior aging at $H_i = 350$ Oe for 1000 s. Curve: fitting with the power-law dependence $R(t) = R_0 + At^{-c}$, $R_0 = 3.496 \Omega$, $A = 0.011$, $c = 0.081$. Inset: $R - R_0$ vs t plotted on the log-log scale. (b) Seven sequential aging cycles at $H_f = -500$ Oe, as labeled, each preceded by aging at $H_i = 350$ Oe for 1000 s. (c,d) c (c) and R_0 (d) vs aging cycle, immediately after cooling from RT. Error bars show the fitting uncertainty.

tonic decrease with decreasing T not affected by the onset of EB low temperatures [Fig. 1(b)], confirming that the AF layer did not directly contribute to the magnetoelectronic signals. Measurements described below were performed with field perpendicular to current [$\theta = 0$].

To establish EB¹⁰, the sample was cooled from RT at $H = 500$ Oe. When varying H , $R(H)$ exhibited sharp peaks at the coercive fields H_- , H_+ [Fig. 1(c)]. The MR observed in the hysteresis loop is close to $\Delta R = 0.28\Omega$ at 5 K, indicating that the reversal of the Py magnetization \mathbf{M} occurs through the configuration almost homogeneously transverse to \mathbf{H} , consistent with a high spatial uniformity of the magnetic properties. The dependencies of the EB field $H_E = -(H_+ + H_-)/2$ and of the coercivity $H_C = (H_+ - H_-)/2$ on T [Fig. 1(d)] are consistent with previous studies^{11–14}.

To investigate the temporal evolution of the magnetization state, H was ramped at a rate of 2 kOe/s from the initial value H_i above H_+ [or below H_-] to the final value H_f below H_- [or above H_+], and subsequently R was recorded in 1 s time increments, with the lock-in time constant set to 100 ms. The evolution of R with time, as shown in Fig. 2(a), was observed over a wide range of T and H_f . Magnetic aging in F/AF heterostructures has been previously mostly discussed in terms of the Arrhenius activation, which can be described by the exponential decay $R(t) = R_0 + R_1 \exp[-t/\tau]$ over the characteristic time $\tau \propto \exp[E_0/kT]$ ^{15,16}. Here, k is the Boltzmann constant, and E_0 is the activation energy. How-

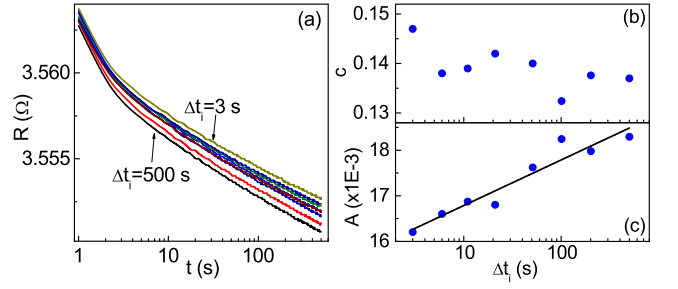


FIG. 3: (Color online) (a) R vs t at $T = 5$ K, $H_f = 150$ Oe, after prior aging at $H_i = -300$ Oe over the time intervals $\Delta t_i = 500$ s (bottom curve), 200 s, 100 s, 51 s, 21 s, 11 s, 6 s, and 3 s (top curve). (b) c vs Δt_i . (c) Symbols: A vs Δt_i , line: logarithmic fit to the data.

ever, our data could not be adequately fitted with exponential decay. One can assume a certain distribution of activation barriers, providing additional fitting parameters^{17,18}. Such a distribution represents a Laplace transform of the time dependence, and thus can be generally expected to yield a good fit to any aging dependence.

In the extreme limit such as encountered at critical points in phase transitions, the absence of the characteristic scale results in power-law dependencies of physical properties on the control parameters¹⁹. Indeed, power-law dependence $R(t) = R_0 + At^{-c}$ provided an excellent fit for our data, confirmed by the linear dependence on the log-log scale [inset in Fig. 2(a)]. We note that this result is consistent with the power-law decay of EB commonly observed in consecutive hysteresis loop measurements, usually described as the training effect²⁰. For a distribution described by the Arrhenius law, a large (small) exponent c indicates the dominance of small (large) activation barriers, while A characterizes the fraction of the system involved in aging.

The results of aging measurements depended on the previous aging history, reminiscent of the training effect^{5,21}. Figure 2(b) shows the results of seven consecutive aging measurements performed following an identical pre-aging procedure, which consisted of applying $H_i = 350$ Oe over time $\Delta t_i = 1000$ s. The first measurement was performed immediately after field-cooling from RT to 5 K. While the power-law exponent c exhibits only a modest irregular dependence on the aging cycle [Fig. 2(c)], the characteristic values of R , and in particular its asymptotic value R_0 , exhibit a monotonic increase [Fig. 2(d)]. This result indicates that the state reached at large t is dependent on the magnetic and thermal history, reminiscent of the kinetic trapping in glassy systems^{22,23}. The results described below were obtained after several prior aging cycles, when the aging characteristics mostly stabilized.

If we assume that the studied system can be described by some distribution of independent activation barriers, then at long aging times it should always reach the same equilibrium state that is independent of its prior his-

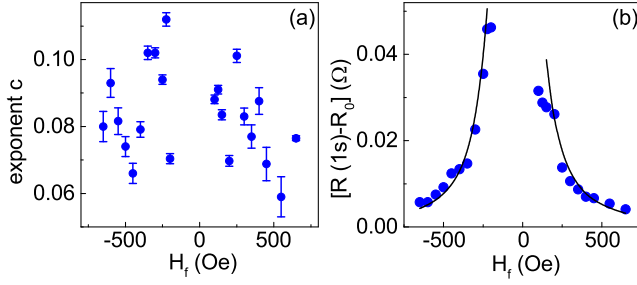


FIG. 4: (Color online) Dependence on H at $T = 5$ K. The duration of aging for both field directions was 1000 s, with $H_i = 350$ Oe (-500 Oe) for $H_f > 0$ (< 0). (a) c vs H . Error bars show the fitting uncertainty. (b) Symbols: $R(t = 1\text{ s}) - R_0$ vs H . Curves: fitting of the $|H| > 200$ Oe data, based on the effective exchange field model described in the text.

tory, which is inconsistent with the data of Fig. 2. Thus, the relaxation in the studied system likely cannot be described by the Arrhenius activation. To further test this conclusion, we consider an experiment that consists of applying filed H_i over a short time Δt_i , followed by the field reversal and subsequent measurement of aging. In the Arrhenius activation model for some distribution of independent subsystems, most of the subsystems with long activation times $\tau \gg \Delta t_i$ are not activated during the short time Δt_i , and consequently do not contribute to the subsequent aging. Thus, Arrhenius aging would reveal a reduced amplitude of the long-time tail of $R(t)$, resulting in a larger decay exponent c or a deviation from the power law.

We performed measurements with Δt_i varied from 500 s to 3 s [Fig. 3(a)]. All the aging curves were well described by the power-law decay, with the same exponent c within the $\approx 10\%$ data spread [Fig. 3(b)]. Together with the dependence of the asymptotic behaviors on the magnetic history, this result demonstrates that aging involves cooperative processes that couple multiple activation energy scales, and thus cannot be described by the Arrhenius law with any distribution of barriers.

While the exponent c was independent of Δt_i , the decay scale A decreased by about 15% when Δt_i was decreased by two orders of magnitude [Fig. 3(c)]. One can expect that A should vanish when Δt_i becomes smaller than the shortest activation times in the system. The approximately logarithmic empiric dependence in Fig. 3(c) extrapolates to $A = 0$ at $t = 10^{-4}$ s. Thus, activation timescales likely span at least seven orders of magnitude, from 10^{-4} s to at least the measurement time of 10^3 s. We note that extrapolation of aging characteristics to $t = 10^{-4}$ s does not lead to unphysical results. For instance, the total estimated variation of resistance, $R(t = 10^{-4}\text{ s}) - R_0 = 10^{4c}A$, did not exceed 0.12Ω in all the aging experiments at 5 K. It is smaller than $\Delta R = 0.28 \Omega$ at this temperature.

Domain wall motion and/or magnetic domain activation in both F and AF can contribute to aging. To es-

tablish the relative contributions of these layers, we studied the dependence on the field H_f . The Zeeman energy should result in the exponential dependence of activation in F on H_f , while for the AF the dependence of aging on H should be weak. Figure 4(a) shows the exponent c for aging at different H_f ranging from -650 Oe to 650 Oe. The resistance variations became too small for reliable measurements at $|H_f| > 650$ Oe. The values of c exhibit random variations around the average $c = 0.084$, and no correlation with H_f . Thus, aging involves activation processes in AF that are not directly influenced by H . The error bars in Fig. 4(a) reflect only the fitting uncertainty, but do not account for the additional errors caused by the transient fields at small t , or aging while H is being ramped.

While the power-law exponent was independent of H_f , the relaxation scale decreased with increasing H_f . In Fig 4(b), we plot the difference between the first measured resistance value at $R(t = 1\text{ s})$ and the asymptotic value R_0 at large t , determined from the fitting. The dependence in Fig. 4(b) is consistent with aging that occurs entirely in the AF layer. Specifically, the exchange experienced by F at the interface with AF can be described by the effective field \mathbf{H}' with average time-dependent components H'_\parallel , H'_\perp in the direction of H and perpendicular to it, respectively. The average angle formed by \mathbf{M} relative to \mathbf{H} is $\phi \approx H'_\perp / (H + H'_\parallel)$, and the corresponding resistance

$$R = R_{min} + \frac{\Delta R}{2} \left[\frac{H'_\perp}{H + H'_\parallel} \right]^2, \quad (1)$$

where R_{min} is the resistance minimum at $\phi = 0$. Our model is supported by the excellent agreement of the fit based on Eq. (1) with the R vs H dependence [curves in Fig. 1(c)], yielding $H'_\perp = 148.5 \pm .5$ Oe from two independent fits of both hysteresis loop branches up to the switching points. It would be less meaningful to fit the same curves beyond the switching point, because of the aging that occurs concurrently with this measurement. Using the form of Eq. (1) to analyze the dependence of the relaxation magnitude on H_f in Fig. 4(b), we obtain a good fit for all the $|H| > 200$ Oe data, with $H'_\parallel = 50$ Oe, $\Delta H'_\perp = 105$ Oe [curves in Fig. 4(b)]. Here, $\Delta H'_\perp$ is the overall reduction of H'_\perp due to the aging at $t > 1$ s. Thus, the dependence of the aging curves on H_f can be explained entirely by the effect of H on M , while its direct effect on the aging process itself is negligible.

Behaviors similar to those discussed above for $T = 5$ K were observed at higher T , extending significantly above $T_B = 140$ K [see Fig. 5(a) for the 210 K data]. To quantitatively characterize the dependence on T , aging was measured with H_f adjusted so that the corresponding value resistance on the R vs H curve was approximately larger than its minimum value by about $0.2\Delta R$ [Fig. 5(b)]. The exponent c exhibited an increase from 0.08 at 5 K to about 0.2 at 200 K [Fig. 5(b)]. Increased random variations of c at higher T can be correlated with

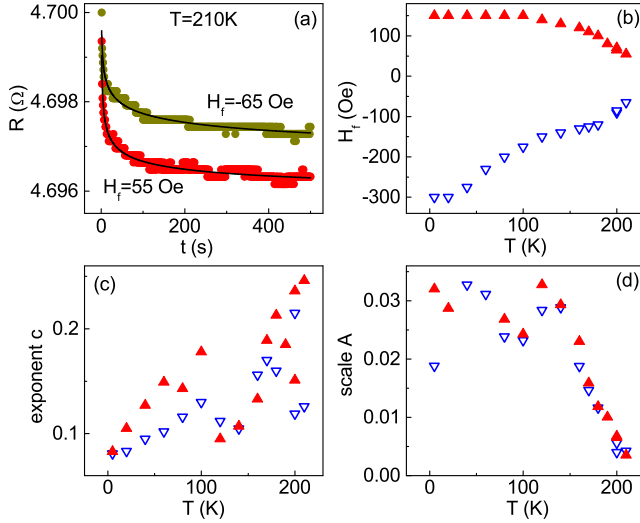


FIG. 5: (Color online) (a) Symbols: R vs t at $T = 210$ K, $H_f = -65$ Oe and $H_f = 55$ Oe, as labeled. Curves: fittings using the power-law dependence with $c = 0.126$ and 0.246 , respectively. (b) H_f vs T used in the aging measurements. (c,d) c (c) and A (d) vs T . Filled (open) symbols are for $H_f > 0$ [$H_f < 0$].

the decrease of A at $T > T_B$ [Fig. 5(d)], which resulted in increased uncertainty and prevented reliable measurements at $T > 210$ K. The increase of c with increasing T is consistent with the larger relative contribution of fast activation processes. Nevertheless, the power-law form of aging curves indicates a non-negligible contribution from the activation times $\tau \approx 1000$ s even at 210 K. The existence of residual aging effects above T_B complements prior observations of AF-induced anisotropy in F even above the Neel temperature of AF²⁴.

Summarizing our main findings, magnetoelectronic measurements reveal aging in thin-film F/AF=Py/FeMn bilayers over a wide range of temperatures. The aging curves exhibit simple scaling with the applied magnetic field, demonstrating that the activation processes are confined to the AF layer. Aging is characterized by the power-law dependence on time and a weak dependence on temperature, indicating a wide range of the activation energies, and the range of activation times that

at $T = 5$ K is estimated to extend over at least seven orders of magnitude, from 10^{-4} s to at least the longest measurement time of 10^3 s. Finally, the same power-law aging exponent is preserved independent of the magnetic history, indicating that aging is a cooperative process, and cannot be described by some distribution of subsystems characterized by the Arrhenius law.

The observed cooperative multiscale aging characterized by the power-law time dependence is reminiscent of the self-organized criticality and the associated avalanche dynamics²⁵. In ferromagnets, such avalanches of magnetic domain reversal are observed as the Barkhausen noise²⁶. In the studied system, activation of a certain AF region can activate or deactivate neighboring regions due to the exchange interaction, resulting in avalanches of AF activation. Since the activation barriers must scale with the volume of the activated regions, and there is no apparent characteristic activation energy in the system, the geometry of the activated AF regions is likely fractal. Further spatially resolved studies, e.g. based on x-ray dichroism microscopy, will likely elucidate the spatial characteristics of activation. Microscopic images in Ref.²⁷ are very conducive of this physical picture. Studies of aging in nanopatterned systems may provide additional information about the characteristic spatial scales of the cooperative phenomena.

Our results may have significant implications for other F/AF heterostructures based on single-crystal and even polycrystalline AF materials, where crystallinity may provide a natural limit for the geometry of the activated AF clusters and cooperativity, but some signatures of the described behaviors will likely remain. F/AF bilayers may also represent a controllable, by means of the magnetic field and temperature, model system that can provide insight into other complex systems that exhibit critical phenomena. For instance, the random effective exchange field experienced by the AF provides an implementation for the Imry-Ma problem of random-field magnetism²⁸, and for which recent simulations indicate the possibility of complex relaxation phenomena²⁹.

We thank Eric Weeks and Stefan Boettcher for helpful discussions. This work was supported by the NSF grant DMR-1504449.

* sergei.urazhdin@emory.edu

¹ L.J. Chen, JOM **57**, 24-31 (2005).

² G. Toulouse, Communication on Physics **2**, 115-119 (1977).

³ D. Mauri, H.C. Siegmann, P.S. Bagus, and E. Kay, J. Appl. Phys. **62**, 3047 (1987).

⁴ A.P. Malozemoff, Phys. Rev. B **35**, 3679(R) (1987).

⁵ C. Schlenker, S.S.P. Parkin, J.C. Scott, and K. Howard, JMMM **54-57**, 801-802 (1986).

⁶ T.K. Yamada, E. Martinez, A. Vega, R. Robles, D. Stoeffler, A.L. Vazquez de Parga, T. Mizoguchi, and H. van Kempen, Nanotechnology **18**, 235702 (2007).

⁷ E. Vincent in *Aging and the Glass Transition*, Springer Lecture Notes in Physics, **716**, Springer, Berlin (2007).

⁸ S. S. P. Parkin, R. F. Marks, R. F. C. Farrow, G. R. Harp, Q. H. Lam, and R. J. Savoy, Phys. Rev. B **46**, 9262(R) (1992).

⁹ See Supplemental Material for the additional deposition, morphological, and crystalline characterization details.

¹⁰ W.H. Meiklejohn and C.P. Bean, Phys. Rev. **105**, 904 (1956).

¹¹ S.S.P. Parkin, V.S. Speriosu in *Magnetic properties of low-dimensional systems II: new developments*, **50**, Springer-

- Verlag (1990).
- ¹² R. Jungblut, R. Coehorn, M.T. Johnson, J. aan de Stegge, and A. Reinders, J.Appl. Phys **75**, 6659 (1994).
 - ¹³ F. Offi, W. Kuch, and J. Kirschner, Phys. Rev. B **66**, 064419 (2002).
 - ¹⁴ S. Urazhdin and C.L. Chien, Phys. Rev. B **71**, 220410 (2005).
 - ¹⁵ E. Fulcomer and S.H. Charap, J. Appl. Phys. **43**, 4190-4199 (1972).
 - ¹⁶ M.D. Stiles and R.D. McMichael, Phys. Rev. B **59**, 3722 (1999).
 - ¹⁷ P.A.A. van der Heijden, T.F.M.M. Maas, W.J.M. de Jonge, J.C.S Kools, F. Roozeboom and P.J. van der Zaag, Appl. Phys. Lett. **72**, 492 (1998).
 - ¹⁸ K. OGrady, L.E Fernandez-Outon, and G.Vallejo-Fernandez, JMMM **322**, 883 (2010).
 - ¹⁹ H.E. Stanley, *Introduction to Phase Transitions and Critical Phenomena*, Oxford University Press, New York (1971).
 - ²⁰ C. Binek, Phys. Rev. B **70**, 014421 (2004).
 - ²¹ T. Hauet, J. A. Borchers, Ph. Mangin, Y. Henry, and S. Mangin Phys. Rev. Lett. **96**, 067207 (2006).
 - ²² D.J. Wales, *Energy landscapes*, Cambridge University Press, Cambridge (2003).
 - ²³ K. Binder and W. Kob, *Glassy Materials and Disordered Solids*, World Scientific, Singapore, (2005).
 - ²⁴ M. Grimsditch, A. Hoffmann, P. Vavassori, Hongtao Shi, and D. Lederman, Phys. Rev. Lett. **90**, 257201 (2003).
 - ²⁵ P. Bak, C. Tang, and K. Wiesenfeld, Phys. Rev. Lett. **59**, 381 (1987).
 - ²⁶ J.S. Urbach, R.C. Madison, and J.T. Markert, Phys. Rev. Lett. **75**, 276 (1995).
 - ²⁷ A. Benassi, M.A. Marioni, D. Passerone and H.J. Hug, Sci. Rep. **4**, 4508 (2014).
 - ²⁸ Y. Imry and S.-K. Ma, Phys. Rev. Lett. **35**, 1399 (1975).
 - ²⁹ T.C. Proctor, D.A. Garanin, and E.M. Chudnovsky, Phys. Rev. Lett. **112**, 097201 (2014).